Zagazig University Medical Journal
www.zumj.journals.ekb.eg
Volume 29, Issue 1, January 2023 https://dx.doi.org/10.21608/zumj.2022.121031.2474
Manuscript ID ZUMJ-2202-2474 (R1)
DOI 10.21608/zumj.2022.121031.2474

ORGINAL ARTICLE

The Role of Lycopene Versus the Normal Capacity of Recovery in A Nanotoxicity Model of The Renal Cortex: An Ultrastructural and Immunohistochemical Study

Enssaf Ahmad Abd Alhameed Ahmad [1]*, Amal AlShahat Ibrahim[1], Ibrahim amin Ibrahim[1] and Wesam El-Said Amin Abdelhamid[1]

[1] Human Anatomy and Embryology Department, Faculty of human Medicine, Zagazig University, Sharkia – Egypt. 44519

*** Corresponding Author**
Enssaf Ahmad Abd Alhameed Ahmad
Human Anatomy and Embryology Department, Faculty of human Medicine, Zagazig University
ORCID identifier is 0000-0003-0660-1942

Submit Date	2022-02-12 08:05:04
Revise Date	2022-03-24 22:26:02
Accept Date	2022-04-19 22:40:58

ABSTRACT

Background: Recently Titanium dioxide nanoparticles (TNPs) are widely used in different fields as in medicinal and daily life purposes. Currently, high concerns have been directed to reveal TNPs toxicity in humans. A dietary carotenoid called lycopene, reported as a powerful antioxidant, is suggested to have a protective rule.

The aim of this study: is to evaluate the reversibility of TNPs toxicity on the renal cortices of adult male albino rats and to clarify protective role of concomitantly administrated lycopene.

Material and methods: Forty-eight adult male albino rats were divided equally into 4 groups;**(I, control group) -Ia,** rats received only regular diet and water for14 days and **Ib,** rats that were injected with 1 ml intra-peritoneal (IP) distilled water daily for14 days**. (II group)**: received IP injection of *TNPs (300 mg/kg)* for14 days**. (III group):** received 10mg/kg daily lycopene for 7 days by gavage then IP injection of TNPs (300 mg/kg) daily for 14 days together with10mg/kg lycopene by gavage. **(IV group):** received IP injection of TNPs (300 mg/kg) daily for 14 days followed by another 14 days of balanced diet only without TNPs or lycopene. By the end of the experiment renal cortices specimens were processed for light microscopic, immunohistochemical and transmission electron microscopic (TEM) study.

Results:
Marked histopathological changes detected in II group were obviously avoided in the III group. While the IV group did not show significant statistical improvement.

Conclusion
TNPs induce pathological ultrastructural changes in rat's renal cortex, that were ameliorated by co-administration of Lycopene.

Keywords: Glomerular Endothelial Cells, Tubules, Immunohistochemical Examination, Nanotoxicity, Albino Rats, Carotenoids, filtration slits

INTRODUCTION

Nanotechnology, which refers to the precise manipulation of matter at the nanometer scale, has revolutionized the commercial application of products in medication, industry, engineering, and environmental tools **[1].**

The rapid advance of nanotechnology resulted in widespread application of nanomaterials; it is used in electronics, some commercial materials and as a component of some drugs **[2].** Exposure of human being to nanoparticles progressively increase everyday creating a major danger to environment and human heath **[3].** Several studies documented serious effects on the human health due to the commonly used nanomaterials in various fields **[4].** Titanium dioxide nanoparticles (TNPs) is one of the most famous produced nanomaterials all over the world, it represents 70% of the pigments' total generation volume around the world and is one of the 1st five nanoparticles utilized among customers **[5-7]**. According to **Frazer [8], Food and Drug Agency [9]** and others **[10,11]** Titanium dioxide is being utilized as shade to brighten skim milk, as food color added substance -but not more than 1% of body weight, food contact substance in food package, all white toothpaste, drugs, pharmaceuticals, makeup as sunscreens and in the field of medicine, it is widely used in synthesis of implanted medical procedures.

Inhalation and dermal contact in the work environment are the most common routes of exposure that cause most of the toxicological

impacts **[12].** According to **Zhao and Castranova [13],** subcutaneous or intravenous infusion of TNPs transporters in nanomedicine are other ways of exposure. Oral route was also reported during utilization of toothpaste, colorants food additives, dietary supplements and even in gums, candies, and sweets **[14].**

The nephron -the kidney's very qualified cells- functions in removal and discharge of any hazards, toxic materials and drugs that enter the human body. This cause the kidney to be one of the most vulnerable organs to the chemical induced toxic effects. It moreover is considered to be one of the most susceptible organs to the impact of TNPs as a result of their filtration through uriniferous tubules **[15].**

L'Azou et al. [16] documented that exposure to high levels of TNPs caused apoptosis of renal tubular cells, interstitial nephritis, and defective kidney function. These hazardous effects occurred through the release and accumulation of reactive oxygen species **[17,18].** Other studies reported inflammation, necrosis of nephric tissues and differentially expressed proteins in the kidneys **[19,20].**

Recently several studies directed great attention to encourage the use of antioxidants -derived from natural sources- in human diet to act as a protector against such health hazards **[21].**

Carotenoids have been widely used as antioxidant dietary supplementations, they have the ability to regain the optimal balance and strengthen the endogenous capacity of human body to use its powerful antioxidant activities**.** Lycopene is one of the powerful cancer prevention agents among dietary carotenoids. It also has many pharmacological and biological activities, for example anti-inflammatory, antioxidant, anti-fibrotic and act as a guard against chemical induced destruction to both renal and hepatic tissues**.** It is found in watermelon, tomatoes, pink grapefruit, papaya, and pink guava. The human body cannot produce carotenoids, so diet is the main source for body tissues and organs. **[22-26]**

This study aims to evaluate the possible protective role of Lycopene against TNPs toxicity on the kidneys and whether these toxic changes are reversible or not.

MATERIALS AND METHODS

Animals:

Forty-eight healthy adult male albino rats were included in this study, weighed 180 to 200g, from the animal house of Zagazig Scientific and Medical Research Center (ZSMRC). They were kept in the animal house for seven days at room temperature in plastic cages with 12-hour light/dark cycles to be acclimatized to the new environment before the experiment. All experimental procedures were performed in accordance with the guidelines of the Institutional Animal Care and Use Committee of Faculty of Medicine; Zagazig University; Egypt (Approval number: ZU-IACUC/3/F/196/2019). These guidelines comply with The Code of Ethics of EU Directive 2010/63/EU for the use of laboratory animals.

Chemicals:

Titanium dioxide nanoparticles (TNPs): Nano-powder with the following characters: <100 nm particle size, surface area of 35-65 m^2/g and purity ≥99.5% trace metals basis. Its CAS No is 634662. It is white odorless fine powder mixture of rutile and anatase. It was manufactured by Sigma-Aldrich chemical Company, Germany and purchased from Sigma-Egypt.

Lycopene: lycopene powder was manufactured by Sigma-Aldrich chemical Company, Germany and purchased from Sigma-Egypt. Its code is c 9750.

Corn oil: obtained from SEKEM co., Cairo, Egypt.

Experimental methods and dosing:

The animals were randomly allocated into four groups as follows:

Control group (I): this group was further subdivided into subgroups:

Subgroup Ia: received balanced diet and water for 14 days and was kept as a **(negative control).**

Subgroup Ib: injected with 1 ml intra-peritoneal (IP) saline daily for 14 days and was kept as a **(positive control).**

Subgroup Ic: received 1 ml corn oil by gavage daily for 14 days and was kept as a **(positive control).**

The treated group (II) (TNP group): this group received IP injection of (TNPs), 300 mg/kg, dissolved in 2ml saline as a single daily dose for 14 days **[27].**

The protective group (III) (TNP and Lycopene group): received a dose of 10mg/kg lycopene dissolved in 1ml corn oil **[28]**, alone, by gavage once daily for the first 7 days then in the following 14 days, IP injection of TNPs (300 mg/kg) dissolved in 2ml saline as a single daily dose was added**.**

Recovery group (IV): received IP injection of TNPs (300 mg/kg) dissolved in 2ml saline as a single daily dose for 14 days followed by another 14 days of balanced diet only without TNPs or lycopene.

At the time of sacrifice, animals of all groups were anesthetized by thiopental inhalation. Laparotomy was performed and the kidneys were dissected out carefully from each animal to be immediately

processed for histological, immunohistochemical and ultrastructural examination by transmission electron microscope (TEM).

Histopathological Examination:

Hematoxylin and Eosin staining:

kidney specimens from all groups were collected at the end of the experiment. The samples were fixed in Bouin's solution, then dehydrated in ascending grades of alcohol, cleared in xylene, and embedded in paraffin. Sectioned (5 µm thickness) and placed onto glass slides. The slides were stained by hematoxylin and Eosin (H&E) to be examined for histopathological details **[29].**

Immunohistochemistry and Morphometric studies:

Caspase-3 Immunohistochemical staining for detection of apoptosis which appeared as brownish cytoplasm of the cells. The primary monoclonal antibody was the rat monoclonal primary antibody to caspase-3 (Ab-7, Mouse Mab. MS.). Immunohistochemical study was performed utilizing the avidin - biotin peroxidase technique **[30].** Caspase-3 immuno-stained sections were morphometrically analyzed. The area percentage of immune reaction to caspase 3 was measured within 9 fields for each rat at a magnification (x400) using image analysis software (National Institute of Health; NIH, Bethesda, MD, USA) **[31].**

Preparation of specimens for transmission electron microscopy:

The specimens from all groups were fixed directly in 2.5% buffered glutaraldehyde solution at pH 7.4, till they were processed according to **[32].** Semithin sections (0.5-1 µm thick) were stained with toluidine blue to select the proper sites for ultrathin sections (70–90 nm thick), double stained with uranyl acetate and lead citrate and examined using a transmission electron microscope (TEM)**.** These sections were examined and photographed by Sumy Electron Optics, P E M - 1 0 0 transmission electron microscope (TEM) in electron microscope research laboratory (EMRL), Faculty of medicine, Al-Azhar University.

Statistical analysis

The parameters for all groups were expressed as mean ± standard deviation (X±SD). The data were subjected to SPSS program. Statistically significant difference was determined by one-way analysis of variance (ANOVA), followed by post hook test, for comparison between different groups **[33].**

RESULTS

Group I (Control group):

Hematoxylin and eosin (H&E):

There were no histological differences between control subgroups as they all showed normal renal cortex, with intact glomeruli surrounded by Bowman's capsule. The latter had normal visceral and parietal layers separated by Bowman's space. Regarding the tubules, the proximal convoluted tubules were lined by a single layer of tall cubical cells with a well-developed brush border occluding mostly the tubular Lumina. The distal convoluted tubules appeared wider and clearly defined due to absence of the brush border **Fig (1A).**

Transmission electron microscopy:

The proximal tubular epithelial cells appeared resting on distinct basement membrane. The tubular cells had large, basal, rounded nuclei with prominent nucleoli and dense clumps of peripheral chromatin condensation (heterochromatin). The basal part of the cells showed numerous basal enfoldings with long rod-like mitochondria oriented parallel to the cell axis and perpendicular to the basement membrane. The apical region of the tubular cells showed numerous closely packed microvilli in a sieve-like pattern forming the brush border which appeared along the tubular lumen. Similarly, the epithelial cells lining distal convoluted tubules rested on clear regular basement membrane which showed some regular basal enfoldings. The cells lateral borders have few interdigitations. Central rounded euchromatic nuclei, basal mitochondria and few luminal short, scattered microvilli appeared at the apical cell border. **Fig (1B, C**).

The renal corpuscles showed several capillary loops. These loops were lined by thin layer of fenestrated endothelial cells. The podocytes could be seen with their long primary and many short secondary foot processes. Bowman's spaces appeared normal and clear of cellular debris. The filtration slits are laid on a regular glomerular basement membrane. The filtration barrier showed obvious three layers: 1) fenestrated endothelium of the glomerular capillaries, 2) the fused basal lamina of the endothelial cells and 3) fenestrations between podocytes' secondary foot processes. **Fig (1D, E**).

Group II (TNP treated group):

Hematoxylin and eosin (H&E):

This revealed variable histological parenchymatous changes. **Fig (2)**. Some renal blood vessels appeared with distorted endothelial cells associated with peri-vascular cellular infiltration, and large areas of interstitial hemorrhage. Numerous tubular dilatations with peri-tubular or interstitial mononuclear cellular infiltrations were detected. Most tubules showed desquamation of their lining cells in the form of intraluminal homogenous acidophilic cellular

debris. Some tubular cells appeared with dark stained pyknotic, rounded or flat nuclei while others showed cytoplasmic degeneration or vacuolations of their cells. A consequent widening of the renal lumens was also detected. **(Fig 2a)**. Concerning the glomeruli, several pathological lesions appeared in renal corpuscles. Some appeared hyper-cellular and congested with obliteration of their Bowman's spaces (**Fig 2b),** others appeared Atrophic or hypo-cellular, divided or separated and also there were glomeruli compressed to the sides of Bowman's capsule leading to widening of the Bowman's spaces. (**Fig 2c).**

Transmission electron microscopy:

Histopathological alterations were seen in almost all components of the renal cortex. The epithelial cells lining convoluted tubules showed varying nuclear shapes; either flat irregular shaped nuclei, indented and heterochromatic shrunken nuclei or rounded central euchromatic nuclei. Most of apical cell borders showed absent or scattered microvilli. Numerous endocytotic vesicles were obvious as well as numerous darkly stained lysosomes of different sizes. Few basal infoldings with polymorphic coalesced mitochondria were noticed. Basement membrane became thick in areas while destructed ill-defined with irregular shape in others**.** As regard the interstitium, it showed excess amounts of collagen fibers and fibroblasts, mononuclear cellular infiltrates, and large areas of hemorrhage **(Fig 3).**

The outer parietal cell layer of Bowman's capsule showed irregular shaped nuclei surrounded by abundant collagen fibers. Glomerular capillaries showed heterochromatic indented nuclei and lacked their fenestrated endothelium. Podocytes appeared with marked indented nuclei, short thick primary processes while other foot processes appeared distorted, fused with obliteration of filtration slits. The glomerular basement membrane was irregular with areas of thickening **(Fig 4).**

Group III (lycopene protected group):

Hematoxylin and eosin (H&E):

In the majority, the renal cortex showed apparently normal glomeruli with reduced Bowman's space. Apparently normal proximal and distal convoluted tubules with normal vesicular nuclei were obvious, except for minimal cytoplasmic vacuolations and some darkly stained nuclei. The superficial parts of some tubular cells rendered their nuclei bulging into the lumen. **(Fig 5a)**

Transmission electron microscopy:

Renal corpuscles appeared normal with their glomerular capillaries. The epithelial lining in most of the convoluted tubules were normally arranged. There were normal euchromatic nuclei with clumps of heterochromatin except for few cells that still have apoptotic nuclei. The cytoplasm was occupied with basal long mitochondria occupying the basal infoldings. All epithelial cells rested on clear regular basement membrane. Endothelial cell cytoplasm shows few mitochondria and endoplasmic reticulum. **(Fig 5B, C)**

Group IV (Recovery group):

Hematoxylin and eosin (H&E):

There were variety of abnormal renal corpuscles; some with wide Bowman's spaces, some were hyper-cellular with obliteration of their Bowman's space, some were atrophied while others were apparently normal. The renal tubules showed normal lining epithelium with vesicular nuclei, but others showed exfoliated nuclei, darkly stained nuclei and minimal cytoplasmic vacuolations. Few mononuclear cellular infiltrations and also signs of mitotic activity were noticed. Some tubules showed dilation and intra-luminal acidophilic cellular debris **(Fig 6A)**

Transmission electron microscopy:

There were histopathological alterations in almost all components of the renal cortex. Some epithelial cells lining the convoluted tubules appeared with no nuclei, while others showed few euchromatic rounded nuclei. Cells appeared bulging in the lumen. An irregular basement membrane of tubules was noticed**.** Some convoluted tubules revealed numerous darkly stained lysosomes and small endocytotic or cytoplasmic vesicles with loss of nuclei in their lumen. Some regions of the apical border appeared with interrupted microvilli, but most of the apical regions showed absent brush border. Basal polymorphic mitochondria were detected. **(Fig 6B, C).**

Glomerular capillaries appeared highly congested with numerous mesangial cells and irregular or indented nuclei. Podocytes appeared with irregular, heterochromatic indented nuclei, while others appeared with vacuolated abnormal nuclei. Lysosomes or residual bodies were obvious in their cytoplasm. Also, irregular thick primary podocyte processes were detected. Some of the pedicels or secondary process appeared distorted or fused with obliteration of the filtration slits and others appeared normal with irregular thickening of glomerular basement membrane. **(Fig 6D, E).**

Immunohistochemical staining of caspase 3: Fig (7)

Group I **(Control group)** showed negative caspase-3 expression in all ductal cells and renal corpuscles with very few, faint positive expression **(Fig. 7a).** In group II **(TNP treated group)**, a strong positive caspase-3 expression was detected in the cytoplasm of numerous tubular cells, some glomerular cells and in few nuclei **(Fig 7b),** while in group III **(lycopene**

protected group) only faint or weak positive caspase-3 expression was noticed (**Fig 7c).**Group IV **(Recovery group),** on the other hand, showed strong positive caspase-3 expression in the cytoplasm of some tubular cells, some glomerular cells and in numerous nuclei. **(Fig 7d)**

Morphometrical analysis:

The mean area % of caspase-3 immunostaining for all groups was represented in tables (1,2) and **Fig (8)**. There was statistically significant difference between different groups in area % were a significant decrease (P< 0.01) in caspase-3 immunostaining was detected in group I &III compared with group II&IV.

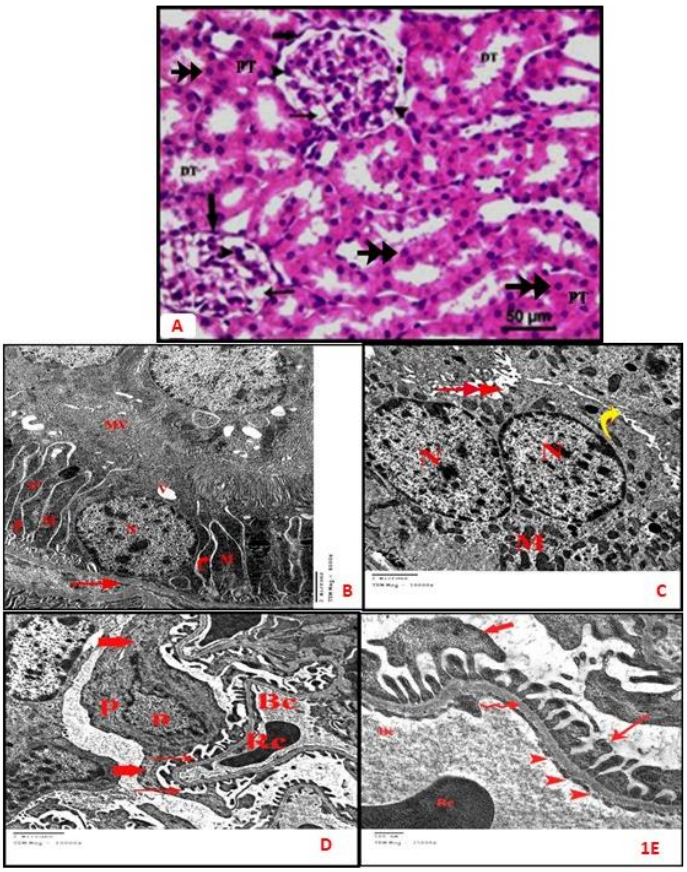

Figure (1): photomicrographs of sections in the renal cortex of a control adult male albino rat; **(pic A; H&E, ×400)** shows normal renal glomerulus **(thin arrow)**, visceral layer of Bowman's capsule **(arrowhead)**, regular parietal layer of flattened attenuated cells **(thick arrow)**, urinary or Bowman's space **(star)**, proximal convoluted tubules **(PT)** with narrow lumen, distal tubules **(DT)** with wide lumen. The lining epithelium of both tubules are cuboidal cells with rounded vesicular nuclei **(double arrow)**. **(Pic. B; TEM. Mic. x8000)** the electron micrograph shows proximal tubular epithelial cells with distinct basement membrane **(arrow)**, nucleus **(N)** is large, basal and rounded**.** There are numerous basal enfoldings **(red curved arrow)**, mitochondria **(M)** are long rod-like**.** There are numerous closely packed microvilli **(mv)**, vesicles **(V**) are prominent pinocytotic**. (Pic. C; TEM. Mic. X10000)**: the electron micrograph of distal tubular epithelial cells shows few lateral interdigitations **(yellow curved arrow)**, microvilli **(double arrow)** are few. **(Pic. D; TEM. Mic. x10000 and its magnification pic. E; x25000)** the electron micrograph of a glomerulus shows blood capillary **(Bc)**, red blood cell **(Rc),** large podocyte **(P)**, euchromatic indented nucleus **(n),** primary **(thick arrow)** and secondary foot processes or pedicles **(thin arrow),** fenestrated endothelial cells **(arrowhead),** filtration slits laid on a regular glomerular basement membrane **(zigzag arrow)**.

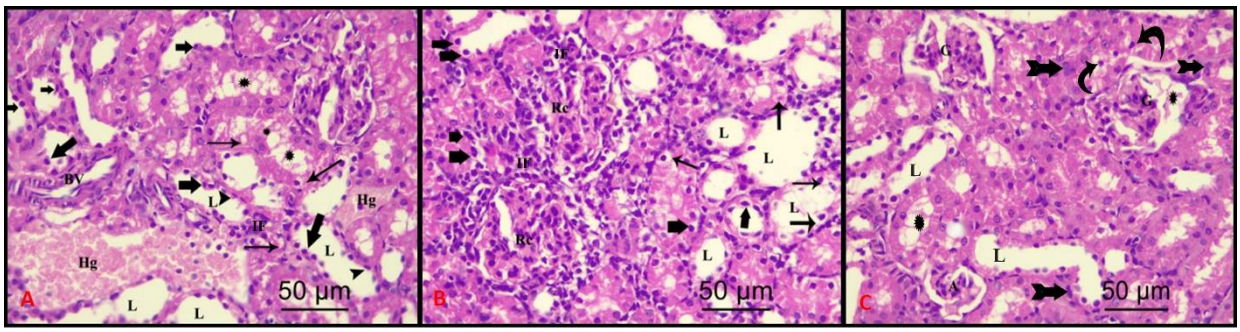

Figure (2): photomicrographs of sections in the renal cortex of TNP treated group of adult male albino rats revealing: blood vessel **(Bv)** is abnormal with distorted endothelial cells**,** vacuolations **(thin arrow)** or cytoplasmic degeneration of the tubular lining cells, numerous tubular dilations **(L),** darkly stained nuclei **(thick arrow),** flat nuclei **(arrowhead)**, interstitial hemorrhage **(Hg)**, acidophilic debris **(star),** peri-tubular or interstitial mononuclear cellular infiltrations **(IF).** Hyper-cellular glomerulus **(Rc)** with obliterated Bowman's spaces. Atrophic or hypo-cellular glomerulus **(A),** divided or separated glomerulus **(G)** with widened Bowman's spaces**,** exfoliated nuclei **(curved arrow)** and signs of mitotic activity **(bifid arrow) (H&E, ×400)**

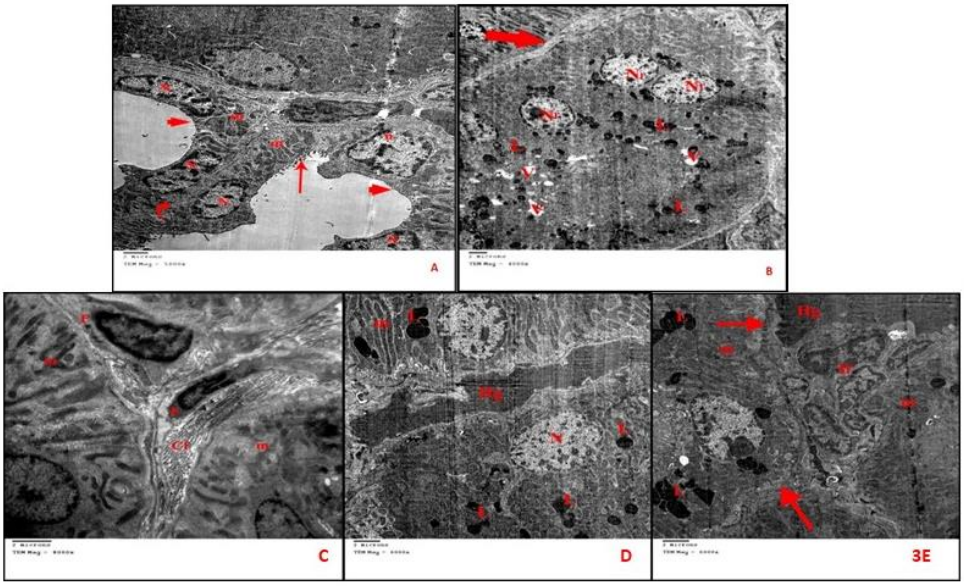

Figure (3): An electron micrograph of an ultra-thin section from the renal cortex of a TNP group. **(Pic. A x5000, pic. B x4000)** show flattened nuclei **(N)**, irregular shaped nuclei **(n)**, polymorphic mitochondria **(m)** within few basal infoldings, absent microvilli **(short arrow)**, scattered microvilli **(thin arrow),** ill-defined basement membrane **(curved arrow)**, rounded central euchromatic nuclei **(Nr),** endocytotic vesicles **(V)** are numerous**,** basement membrane **(arrow)** is thick, and lysosomes **(L)** are numerous darkly stained. **(Pic Cx8000, pic Dx6000, pic Ex6000)** show abundant collagen **(Cf)** and fibroblasts **(F),** large area of hemorrhage **(Hg),** euchromatic nucleus **(N)**, numerous darkly stained lysosomes **(L)**, mononuclear cellular infiltration **(If)**, irregular ill-defined basement membrane **(arrow)**, mitochondria **(m)** is basally arranged polymorphic and coalesced.

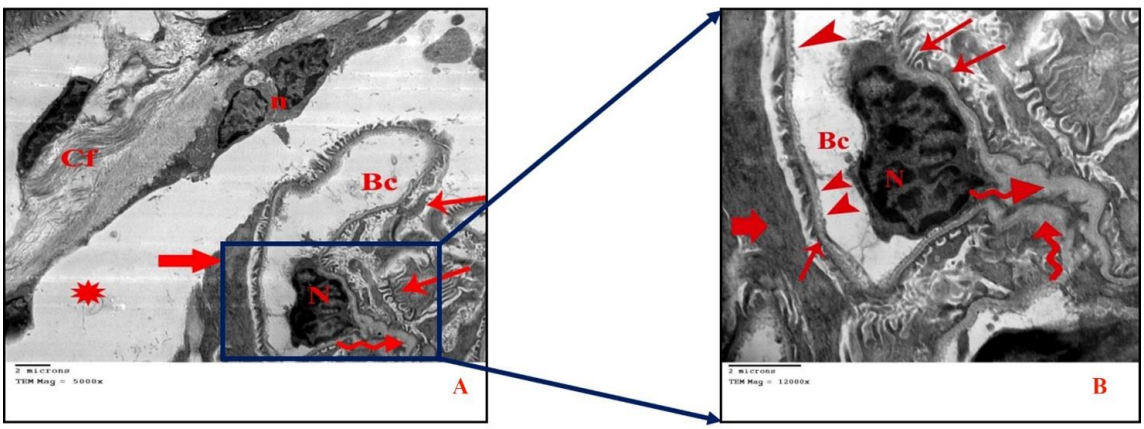

Figure (4): An electron micrograph of an ultra-thin section from the renal cortex of a TNP group showing: glomerular capillary **(Bc)**, heterochromatic nucleus **(N),** irregular shaped nuclei **(n)** of the outer parietal cell layer of Bowman's capsule**,** Bowman's space **(star)**, abundant collagen fibers **(Cf)**. On higher magnification, there is lost fenestrated endothelium **(arrowhead),** thick primary processes of podocyte **(thick arrow)** and distorted, fused foot processes or pedicles **(arrow)** with obliteration of filtration slits in between are also seen. Irregular, thick glomerular basement membrane **(zigzag arrow)** is noticed. **(TEM. Mic., pic. Ax5000, pic. Bx12000)**

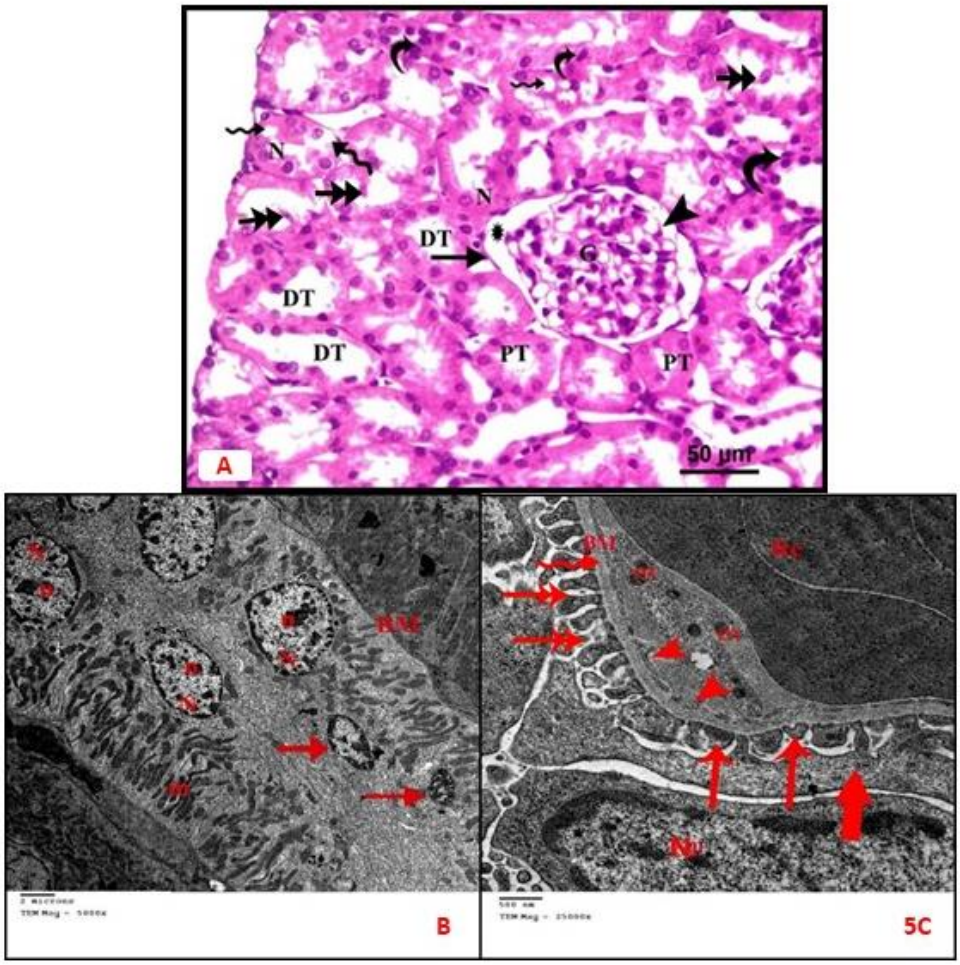

Figure (5): photomicrographs of sections of the renal cortex of a protected group**. (A; H&E x400)** shows apparently normal glomeruli **(G)**, parietal attenuated layer **(arrow)**, normal visceral layer **(arrowhead)**, reduced Bowman's space **(star)**, proximal **(PT)** and distal convoluted tubules **(DT)** are apparently normal, normal vesicular nuclei **(N)**, cytoplasmic vacuolations **(zigzag arrow),** darkly stained nuclei **(curved arrow),** bulging nuclei **(double arrow)** into the lumen of tubules. **(TEM. Mic., pic. Bx5000, pic. Cx25000)**: the electron micrograph; shows convoluted tubules (pic. B) with normal euchromatic nuclei **(N),** clumps of heterochromatin **(n),** apoptotic nuclei **(arrow)**, clear thin regular basement membrane **(BM)**, mitochondria **(m)** are numerous and long**.** The renal glomeruli (pic. C) show blood capillary with red blood cell **(Rc),** mitochondria (**m**) are few**,** endothelium **(zigzag arrow),** regular basement membrane **(BM),** fenestrated endothelium **(arrowhead),** primary long processes **(thick arrow)**, secondary foot processes or pedicles **(thin arrow)** of the podocyte, with euchromatic nucleus **(Np),** filtration slits **(double arrow).**

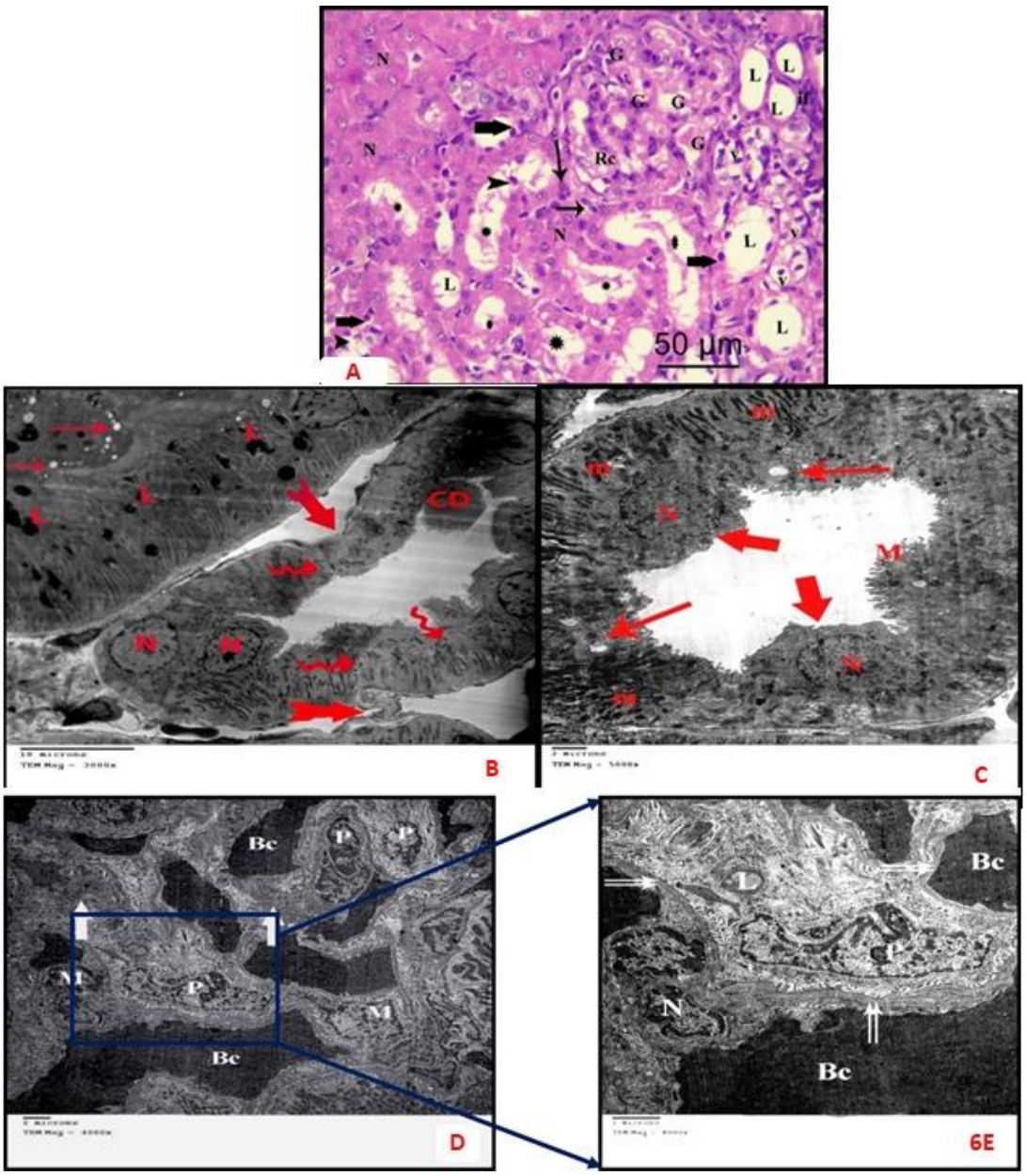

Figure (6): photomicrographs of sections of the renal cortex from a recovery group. **(A; H&E x400)** shows hypercellular renal corpuscle **(Rc)**, congested glomerular capillaries with obliterated Bowman's space **(G)**. Vesicular nuclei **(N)** in normal tubules. Acidophilic cellular debris **(star)** in tubules lumen**.** Exfoliated nuclei **(arrowhead).** Darkly stained nuclei **(thick arrow)**. Extensive cytoplasmic vacuolations **(v).** Apparent luminal dilatation **(L)**. Few peritubular mononuclear cellular infiltration **(If)**. Signs of mitotic activity **(thin arrow). (TEM. Mic., pic. Bx3000, pic. Cx5000):** the electron micrographs show large area of the epithelial cells lining the convoluted tubules with no nuclei **(zigzag arrow)** others show few euchromatic rounded nuclei **(N)**. Some cellular debris **(CD)** appear in the tubular lumen**.** An irregular basement membrane **(bifid arrow)** can be seen. Other convoluted tubules reveal numerous darkly stained lysosomes **(L)** and small endocytic or cytoplasmic vesicles **(thin arrow).** Other areas show apical border with interrupted microvilli **(M)**, and even with absent brush border **(thick arrow).** Also, polymorphic mitochondria are detected **(m). (TEM. Mic., pic. D x4000, pic. E x8000):** the electron micrographs show congested glomerular capillaries **(Bc).** Podocytes with irregular, indented nucleus **(P)**, their processes **(thick arrow)**, numerous mesangial cells **(M)** are observed. On higher magnification**,** mesangial cells appear with irregular or indented nuclei **(N)**, irregular thick fused glomerular basement membrane **(double arrow)**, lysosomes are detected **(L)**.

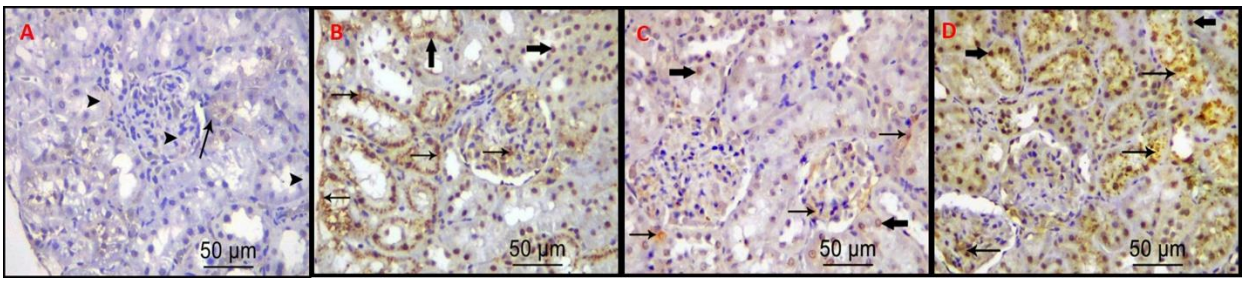

Figure (7): photomicrographs of immunohistochemically stained sections in the renal cortex of adult male albino rats; **control group (A),** showing negative caspase-3 expression in all ductal cells and renal corpuscle **(arrowhead)** with very few faint positive expressions **(arrow)**. **TNPs treated group (B)** showing strong positive caspase-3 expression in the cytoplasm of numerous tubular cells, some glomerular cells **(arrow)** and in few nuclei **(thick arrow). Protective group (C),** showing faint or weak positive caspase-3 expression in the cytoplasm of some tubular cells, some glomerular cells **(arrow)** and in few nuclei **(thick arrow). Recovery group (D),** showing strong positive caspase-3 expression in the cytoplasm of some tubular cells, some glomerular cells **(arrow)** and in numerous nuclei **(thick arrow). (Caspase-3 and has a counter stain, ×400)**

Table (1) : Comparing the means of area percentage of caspase-3 immune reaction among the diffèrent groups using ANOVA test:

Groups	*Control*	*Treated*	*Recovered*	*Protected*	*P*
Area%:	*0.022±0.005*	*24.107±4.959*	*19.335±2.021*	*1.619±0.540*	*<0.001***
Mean ± SD	*0.018- 0.030*	*19.5 – 34.88*	*16.88 - 21.99*	*1.03 – 2.72*	
Range					

*ANOVA: Analysis of variance, SD: Standard deviation, **: highly significant (P<0.01)*

Table (2): LSD for comparing the mean of area percentage of caspase-3 immune reaction among the different groups:

Groups	*Treated*	*Recovered*	*Protected*
Control	*<0.001***	*<0.001***	*0.193 NS*
Treated	-	*<0.001***	*<0.001***
Recovered	*<0.001***	-	*<0.001***

*LSD: Least significant difference, NS: Nonsignificant (P>0.05), **: highly significant (P<0.01)*

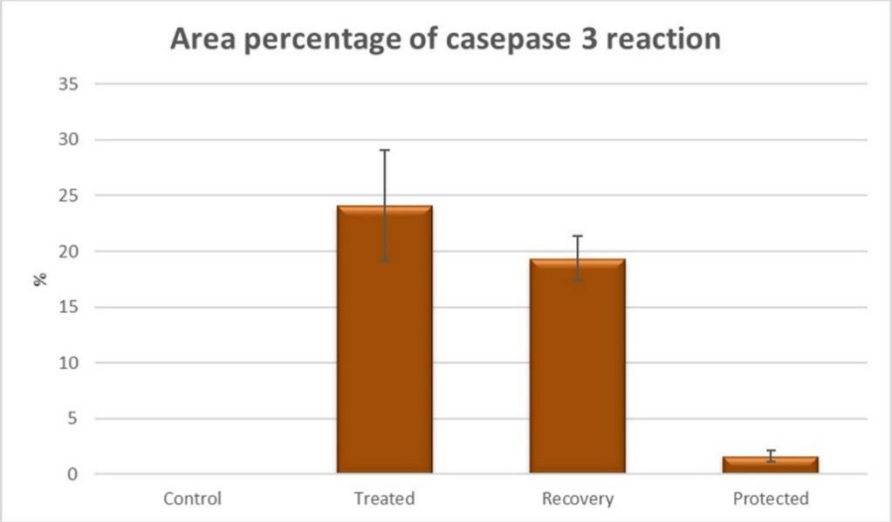

Figure (8): A chart showing mean value of area percentage of caspase-3 immune reaction among the different groups**.**

DISCUSSION

This study has been designed to investigate the potential protective effects of lycopene on the toxic impacts of TNP on the kidneys of adult male albino rat and to detect wither the capacity of spontaneous recovery from such changes are effective or not, as the kidneys are responsible for elimination of wasted and toxic materials from the body, and according to **Pujalté et al. [34]** TNP in the circulation is filtered by renal clearance.

In this study, intra-peritoneal route was chosen for injection of TNP due to its rapid and good absorption owing to the intensive blood and lymph vessels of peritoneum in addition to its large surface area, thus the drug easily reaches the circulation. Also, this injection can avoid the common local gastrointestinal side effects related to oral administration **[35]**.

Lycopene has been recommended for its potent antioxidant effect among dietary carotenoids. Carotenoids have been commonly used as antioxidants, only through dietary supplements because they are cheap, safe, and human body cannot produce them. They play a role in recuperating the optimal balance and strengthening the endogenous antioxidant defenses. **[22,24,26]**

Histopathological examination of TNP treated group revealed varying pathological changes ranging from hyper-cellularity, hypo-cellularity to atrophic renal corpuscles. This clarifies the findings of **Fartkhooni et al.** [**36]** who reported swelling and dilatation of Bowman's capsule**.** Also, according to **Gui et al. [37],** the increased TNP concentrations was associated with significant reduction of number of renal glomeruli and tissue necrosis. **Altayeb et al. [28]** documented several renal histopathological changes associated with dilated congested glomerular capillaries as was obvious in this study.

On ultrastructure study, irregular shaped heterochromatic nuclei were detected in the renal corpuscles coinciding with the findings of **Gui et al. [37]** who reported classical morphology of apoptosis in the renal cells.

The outer parietal cell layer of Bowman's capsule showed abundant collagen fibers ultra-structurally. Also, the interstitium contained excess amounts of collagen fibers, fibroblasts and showed infiltration with mononuclear cellular infiltrates. These findings support number of reports from previous in-vivo and in-vitro studies that related the impaired nephric functions to the induced nephric inflammation **[17,38-40]. L'Azou et al. [16]and Masoud et al. [41]** related the damage to accumulation of reactive oxygen species, while **Kumar et al. [42]** mentioned that TNP increased production of several cytokines and this strongly attracts the leukocytes and other cells which share in the inflammatory reaction, causing subsequent damage to the kidney**.** In the study of **Helmy et al. [15],** they referred to the interstitial fibrosis as an end stage of the sequelae of fluid oozing outside the tubules, edema, and cellular infiltrations. However, they pointed out that fibroblasts may be transformed from the flattened cells lining some tubules.

Regarding renal tubules, degeneration, vacuolations, accumulation of homogenous acidophilic cellular debris and tubular dilation were detected. These go with the results of number of previous studies **[28,36,43].** Light microscopic findings were enforced ultra-structurally as the tubular cells appeared with shrunken irregular nuclei and numerous endocytotic vesicles. The

scattered microvilli and absence of apical cell borders explains the detected tubular dilatation.

Similar to the findings of **Mohamed and Sayed [40],** numerous lysosomes were obvious**.** This was referred to by **Scown et al. [44]** as aggregations of clusters of nanoparticles either collected in lysosomes or surrounding the kidney tubules.

In the present study, renal blood vessels appeared lined with elongated endothelial cells, associated with peri-vascular cellular infiltration and large areas of interstitial hemorrhage and interstitial mononuclear cellular infiltration. These results were in accordance with **Gui et al. [37]** who detected inflammatory cellular infiltration and cell loss along vessel wall. Others reported the presence of interstitial mononuclear cellular infiltration and fibrosis between degenerated tubules and renal corpuscles **[28]**.

Histological examination of lycopene protected group showed marked amelioration of nearly all the histopathological changes produced by TNPs. These results were in agreement with **Li et al.** and others **[28, 45-47]** who reported that most of glomeruli were more or less as that of control on consuming lycopene. Other studies referred this improvement to lycopene's efficient free radical expelling action **[47,48]**. Light microscopic improvement was confirmed on ultra-structural examination except for some isolated cells that showed apoptotic nuclei.

In the current study, histopathological examination of recovery group -both at Light microscopic and ultra-structural levels- revealed the same alterations detected with TNP treated group. This was in contrast to **Mohamed and Sayed [40]** who reported partial improvement in their recovery group. **Also, Fartkhooni et al. [36]** reported compensated pathological changes of kidney tissue. they attributed that to gradual disposal of nanoparticles which had been accumulated in the body. Mostly, these ultrastructure improvements return to their longer recovery period (12 months) after the last dose of titanium and the smaller doses of TNPs used.

In conclusion, this study revealed that TNP induced ultrastructural abnormalities of the kidneys are poorly recoverable at considerable period of time, taking in consideration the unavoidable wide spread of nanotechnology applications. These abnormalities were alleviated by Lycopene Co-administration. Eventually, the study supports the use of lycopene as a potent protective supplement against the toxic effects of TNP.

RECOMMENDATION

Precise precautions should be used in nano technology to gain its benefits and avoid possible drawbacks**.** Limiting the occupational and environmental exposure to TNP is highly recommended whenever possible. Increase awareness about the health hazards caused by food additives as this might be a measure to limit ingestion of TNPs. Additional toxicity studies are needed to elucidate the underling mechanisms of TNPs toxicity. Lycopene supplementations are beneficial for limiting the toxic effects of TNPs on the kidney especially in highly exposed individuals.

Acknowledgement:

The authors are grateful to Zagazig scientific and medical research center (ZSMRC) team for supporting experimentation in their laboratories.

Declaration of interest and Funding information: The authors report no conflicts of interest.

Contributors and Authorship: All the authors listed have contributed to the work, participated in the construction of this manuscript, and approved the final version to be published. All authors agreed to submit the manuscript

REFERENCES

1-Newman MD, Stotland M, Ellis JI. The safety of nanosized particles in titanium dioxide- and zinc oxide-based sunscreens. J Am Acad Dermatol. 2009; 61: 685–692.

2-Emerich DF, Thanos CG. Nanotechnology and medicine. Expert Opin Biol Ther. **2003**; 3: 655–663.

3-Nel A, Xia T, Mädler L, Li N. Toxic potential of materials at the nano level. Science. **2006;** 311: 622–627.

4-Han Y, Xu J, Li Z, Ren G, Yang Z. In vitro toxicity of multiwalled carbon nanotubes in C6 rat glioma cells. Neurotoxicology. **2012**; 33: 1128–1134.

5-Baan R, Straif K, Groose Y, Secretan B, Ghissassi F, Ogliano V. Carcinogenicity of carbon black, titanium dioxide, and talc. WHO International Agency for Research on Cancer Monograph Working Group. Lancet Oncol. **2006;** 4: 295-296.

6-Ortlieb M. White Giant or White Dwarf?: Particle Size Distribution Measurements of TiO2. G.I.T. Laboratory Journal Europe. **2010**;14: 42-43.

7-Shukla R, Kumar A, Gurbani D, Pande AK, Singh S, Dhawan A. Tio2 nanoparticles induce oxidative DNA damage and apoptosis in human liver cells. Inform healthcare. **2013;** 7: 48-60.

8-Frazer L. Titanium dioxide: environmental white knight?. Environmental Health Perspectives. **2001;**109(4): 174-77.

9-Food and Drug Administration. Listing of color additives exempt from certification. In Code of Federal Regulations Title 21-Food and Drugs. 21 CFR 73. 2575. Washington, DC: US Government Printing Office. **2002**

10-**Wang JJ, Sanderson BJ, Wang H.** Cyto- and genotoxicity of ultrafine TiO2 particles in cultured

human lymphoblastoid cells. Mutation Research. **2007;** 628: 99-106.

11-Sul YT. Electrochemical growth behavior, surface properties, and enhanced in vivo bone response of TiO2 nanotubes on micro structured surfaces of blasted, screw-shaped titanium implants. International Journal of Nanomedicine. **2010**; 5: 87-100.

12-Robertson TA, Sanchez WY, Roberts MS. Are commercially available nanoparticles safe when applied to the skin? Journal of Biomedical Nanotechnology. **2010;** 6: 452-468.

13-Zhao J, Castranova V. Toxicology of nanomaterials used in nanomedicine. Journal of Toxicology and Environmental Health Part B: Critical Reviews. **2011;** 14(8): 593-632.

14-Weir A, Westerhoff P, Fabricius L, Hristovski K, Von Goetz N. Titanium dioxide nanoparticles in food and personal care products. Environmental Science and Technolog. **2012**; 46: 2242–2250.

15-Helmy AM, Sharaf-El-Din NA, Abd-El-Moneim RA, Rostom DR. Histological study of the renal cortical proximal and distal tubules in adult male albino rats following prolonged administration of titanium dioxide nanoparticles and the possible protective role of l-carnosine. The Egyptian Journal of Histology. **2015;** 38: 126-142.

16-L'Azou B, Jorly J, On D, Sellier E, Moisan F, Fleury-Feith J, Cambar J, Brochard P, Ohayon-Courtès C. In vitro effects of nanoparticles on renal cells. Part Fibre Toxicol. **2008**; 5: 22.

17-Zhao JF, Li N, Wang SS, Zhao XY, Wang J, Yan JY, Ruan J, Wang H, Hong FS. The mechanism of oxidative damage in nephrotoxicity of mice caused by nano-anatase TiO2. J Exp Nanosci. **2010;** 5: 447–462.

18- Hegazy AA, Enssaf Ahmad, Dalia Ibrahim and Omnia Ahmad. Potential role of Moringa Oleifera in alleviating paracetamol-induced nephrotoxicity in rat**.** Eur. J. Anat. **2020;** 24 (3): 179-191**.** http://www.eurjanat.com/web/paper.php?id=190640ah .

19-Jeon YM, Park SK, Rhee SK, Lee MY. Proteomic profiling of the differentially expressed proteins by TiO2 nanoparticles in mouse kidney. Mol Cell Toxicol. **2010**; 6: 419–425.

20-Gui SX, Zhang ZL, Zheng L, Cui YL, Liu XY, Li N, Sang XZ, Sun QQ, Gao GD, Cheng Z, Cheng J, Wang L, Tang M, Hong FS. Molecular mechanism of kidney injury of mice caused by exposure to titanium dioxide nanoparticles. J Hazard Mater. **2011**: 195: 365–370

21-El-Mahalaway AM, Selim AA, Mahboub FAR. The potential protective effect of propolis on experimentally induced hepatitis in adult male albino rats. Histological and immunohistochemical study. Journal of Histology & Histopathology. **2015**: 2(14): 1-14.

22-Daniel EE, Mohammed A, Tanko Y, Ahmed A. Effect of lycopene on altered kidney antioxidant enzymes activity and functions in streptozotocin induced diabetic Wister rats. Cell Biology. **2015**; 3(1): 1-13.

23-El-Sayed EM, Fouda EE, Mansour AM, Elazab AH. Protective Effect of lycopene against carbon tetrachloride-induced hepatic damage in rats. Int J Pharma Sci. **2015**; 5(1): 875-881.

24-Sweetman SC. Martindale, The complete drug reference. 37th ed., Pharmaceutical Press, UK, and USA. **2011**

25-Sharma S, Vijaya P. Ameliorating potential of lycopene against cadmium toxicity in kidney of albino mice. International Journal of Advanced Research. **2015**; 3(2): 766- 770

26-Yildiz M, Sandikci M. Changes in rat ovary with experimentally induced diabetes and the effects of lycopene on those changes. Rom J Morphol Embryol. **2016**; 57(2): 703- 713.

27-Xu J, Shi H, Ruth M, Yu H, Lazar L, Zou B, Yang C, Wu A, Zhao J. Acute toxicity of intravenously administered titanium dioxide nanoparticles in mice. PLoS ONE. **2013**; 8(8): e70618**.**

28-Altayeb ZM, El Mahala-way AM, Salem MM. Histological and Immunohistochemical Study of Titanium Dioxide Nanoparticle Effect on the Rat Renal Cortex and the Possible Protective Role of Lycopene. Egyptian Journal of Histology. **2017;** 40(1): 80-93.

29-Bancroft J, Gamble M. Theory and practice of Histological technique, (6th Ed). Churchill Livingston, New York, Edinburgh, London. **2008**;165-175**.**

30-Ramos-Vara JA, Kiupel M, Baszler T, Bliven L, Brodersen B, Chelack B, Czub S, Del Piero F, Dial S, Ehrhart EJ, Graham T, Manning L, Paulsen D, Valli VE, West K. Suggested guidelines for immunohistochemical techniques in veterinary diagnostic laboratories. J. Vet. Diagn. Invest. **2008;** 20**:** 393–413.

31-Jensen EC. Quantitative Analysis of Histological Staining and Fluorescence Using Image. J. Anat Rec. **2013;** 296: 378–381, https://doi.org/10.1002/ar.22641

32-Hayat MA. Principles and techniques of electron microscopy. Biological applications. 3rd ed. London: CRC Press. **1989;** 24–74.

33-Dean A, Dean G, Colombier D. Epi-info version 1 for the year 2000 Date Basic Statics and Epidemiology on Microcomputer CDC. Georgia, USA**. 2000**

34-Pujalté I, Passagne I, Brouillaud B, Tréguer M, Durand E, Ohayon-Courtès C, L'Azou B. Cytotoxicity and oxidative stress induced by different metallic nanoparticles on human kidney cells. Part Fibre Toxicol. **2011**; 8: 10.

35-Krinke GJ. The Laboratory Rat, Handbook of Experimental Animals, 1st Edition. Academic Press. **2000**. https://doi.org/10.1016/B978-0-12-426400-7.X5037-7

36-Fartkhooni FM, Noori A, Mohammadi A. Effects of titanium dioxide nanoparticles toxicity on the kidney of male rats. International Journal of Life Sciences. **2016;** 10(1): 65–69**.**

37-Gui S, Sang X, Zheng L, Ze Y, Zhao X, Sheng L, Sun Q, Cheng Z, Cheng J, Hu R, Wang L, Hong F, Tang M. Intragastric exposure to titanium dioxide

nanoparticles induced nephrotoxicity in mice, assessed by physiological and gene expression modifications. Particle and Fiber Toxicology. **2013;** 10: 4

38-Rahman Q, Lohani M, Dopp E, Pemsel H, Jonas L, Weiss DG, Schiffmann D. Evidence that ultrafine titanium dioxide induces micronuclei and apoptosis in Syrian hamster embryo fibroblasts. Environ Health Perspect. **2002**; 110: 797–800.

39-Peters K, Unger RE, Kirkpatrick CJ, Gatti AM, Monari E. Effects of nano scaled particles on endothelial cell function in vitro: studies on viability, proliferation and inflammation. J Mater Sci Mater Med. **2004**; 15: 321–325.

40-Mohamed SH, Sayed HA. Hazards of nanotechnology: Effect of titanium dioxide nanoparticles on the liver and renal cortex of albino rats. An electron microscopic study. The Egyptian Journal of Histology. **2013**; 36: 389- 399

41-Masoud R, Bizouarn T, Trepout S, Wien F, Baciou L, Marco S, Levin CH. Titanium dioxide nanoparticles increase superoxide anion production by acting on NADPH oxidase. PLoS ONE. 2015; e0144829. 10(12), 17.

42-Kumar S, Meena R, Paulraj R. Role of macrophage (M1 and M2) in titanium-dioxide nanoparticle induced oxidative stress and inflammatory response in rat. Appl Biochem Biotechnol. **2016;** 180(7): 1257-1275

43-Zhang Z, Zheng L, Cui Y, Liu X, Li N et al. Molecular mechanism of kidney injury of mice caused by exposure to titanium dioxide nanoparticles. J Hazard Mater. **2011**; 195: 365–370.

44-Scown TM, Aerle RV, Johnston BD, Cumberland S, Lead JR, Owen R, Tyler CR. High Doses of Intravenously Administered Titanium Dioxide Nanoparticles Accumulate in the Kidneys of Rainbow Trout but with no Observable Impairment of Renal Function. toxicological sciences. **2009;** 109(2): 372–380

45-Li W, Wang G, Lu X, Jiang Y, Xu L, Zhao X. Lycopene ameliorates renal function in rats with streptozotocin-induced diabetes. Int J Clin Exp Pathol. **2014**: 7(8): 5008-5015.

46-Kaya C, Karabulut R, Turkyilmaz Z, Sonnez K, Kuluk G. Lycopene has reduced renal damage histopathologically and biochemically in experimental renal ischemia-reperfusion injury. Journal Renal failure. **2015**; 37(8): 1390-1395.

47-Pandir D, Unal B, Bas H. Lycopene protects the diabetic rat kidney against oxidative stress mediated oxidative damage induced by furan. Arch Biol Technol. **2016**;59, e16150794: 1-12.

48-Palabiyik SS, Erkekoglu P, Zeybek ND, Kizilgun M, Baydar DE, Sahin G et al. Protective effect of lycopene against ochratoxin A induced renal oxidative stress and apoptosis in rats. Exp ToxicolPathol. **2013**; 65: 853-861.

ORGINAL ARTICLE
ZAGAZIG UNIVERSITY MEDICAL JOURNAL

To Cite:
Ahmad, E., Ibrahim, A., Ibrahim, I., Abdelhamid, W. The role of lycopene Versus the normal capacity of recovery in a nanotoxicity model of the renal cortex: An ultrastructural and immunohistochemical study. *Zagazig University Medical Journal*, 2023; (91-103): -. doi: 10.21608/zumj.2022.121031.2474